

# A Multi-Survey Machine-Readable Corpus of Milky Way Globular Cluster Parameters for Retrieval-Augmented Generation Applications

David C. Flynn

EPS Research, Laurel, MD 20707, USA

ORCID: 0000-0002-2768-6650

[davidflynn@eps-research.com](mailto:davidflynn@eps-research.com)

Submitted to *Publications of the Astronomical Society of the Pacific*

## Abstract

We present the Milky Way Globular Cluster Corpus v1.3.1, a unified machine-readable database of fundamental parameters for 174 Milky Way globular clusters assembled from four independent published surveys. Each cluster record integrates photometric, structural, and spectroscopically-calibrated metallicity parameters from Harris [1996] (2010 revision), Gaia EDR3 proper motions from Vasiliev and Baumgardt [2021], N-body dynamical masses and orbital parameters from Baumgardt et al. [2023], and mean chemical abundances from the APOGEE DR17 globular cluster Value Added Catalog of Schiavon et al. [2024]. The corpus contains 17,438 non-null data points across 174 clusters stored in JSONL, JSON, and flat CSV formats with consistent native-typed fields (`float`, `int`, `bool`, `null`), embedded provenance blocks, and fully documented schema. Survey coverage is 157/174 clusters for Harris photometry, 170/174 for Gaia EDR3 proper motions, 154/174 for Baumgardt N-body dynamics, and 72/174 for APOGEE DR17 chemistry. The corpus was designed as a Retrieval-Augmented Generation (RAG) knowledge base for large language model applications in astrophysics research, following the same multi-survey integration methodology as the Unified Galaxy HI Rotation Curve Corpus [Flynn, 2026b], and has been validated for structured context injection with instruction-following language models. It is equally suitable for traditional quantitative analyses including orbit modeling, cluster classification, chemical tagging, and

multi-survey cross-validation. The dataset is available at Zenodo DOI: [10.5281/zenodo.19907766](https://doi.org/10.5281/zenodo.19907766).

**Keywords:** globular clusters — Milky Way — stellar kinematics — chemical abundances — N-body models — proper motions — Gaia EDR3 — APOGEE — catalogs — databases — methods: data analysis

## 1 Introduction

The Milky Way globular cluster system is one of the most thoroughly studied populations in astrophysics. These old, dense stellar systems serve as tracers of Galactic structure and chemical evolution, probes of dark matter distribution, and benchmarks for stellar population models. Decades of multi-wavelength observational campaigns have produced a rich but fragmented literature: photometric catalogs, N-body dynamical models, Gaia astrometry, and high-resolution spectroscopic surveys exist as independent publications, each with its own format, naming convention, and coverage.

The rise of large language models (LLMs) and Retrieval-Augmented Generation (RAG) architectures in scientific research creates a new demand: machine-readable corpora that are not merely tabular databases but structured knowledge representations accessible to both programmatic analysis and natural language inference pipelines. A RAG corpus must be consistently typed, null-safe, self-describing, and organized so that each record is a semantically coherent unit — a single cluster carrying all available information about that object from all available sources.

This paper describes the construction and content of the Milky Way Globular Cluster Corpus v1.3.1, which satisfies these requirements. The corpus follows the design principles established in the Unified Galaxy HI Rotation Curve Corpus [Flynn, 2026b], extending the multi-survey integration approach from galaxy kinematics to globular cluster physics.

The four source surveys were chosen to provide orthogonal physical information: Harris [1996] for photometry and classical structure; Vasiliev and Baumgardt [2021] for space astrometry; Baumgardt et al. [2023] for dynamical modeling; and Schiavon et al. [2024] for high-resolution spectroscopic chemistry. No single survey covers all 174 clusters in the corpus; coverage fractions range from 41% (APOGEE DR17) to 98% (Vasiliev & Baumgardt 2021), with the Harris catalog forming the 157-cluster backbone.

## 2 Source Surveys

### 2.1 Harris (1996, 2010 Edition)

The Harris catalog [Harris, 1996], revised 2010, is the standard reference compilation for Milky Way GC parameters, providing photometric and structural data for 157 clusters.

The spectroscopic metallicity  $[\text{Fe}/\text{H}]$  (Carretta et al. scale) entries in the Harris catalog are derived from the homogeneous metallicity scale of Carretta et al. [2009], based on high-resolution ( $R \sim 45,000$ ) UVES optical spectroscopy; they are not photometric estimates. Parameters include: positions in equatorial and Galactic coordinates; heliocentric distance  $R_{\odot}$  and Galactocentric distance  $R_{\text{GC}}$ ; Galactocentric  $X/Y/Z$  coordinates; reddening  $E(B - V)$ ; spectroscopic metallicity  $[\text{Fe}/\text{H}]$  (Carretta et al. scale); apparent and absolute  $V$  magnitudes; distance modulus; horizontal branch magnitude  $V_{\text{HB}}$ ; color indices  $U - B$ ,  $B - V$ ,  $V - R$ ,  $V - I$ ; ellipticity; spectral type; King concentration parameter  $c$  [King, 1966]; core-collapse classification; core and half-light radii in arcmin and kpc; central surface brightness  $\mu_V$ ; central logarithmic density  $\log \rho_0$ ; core and half-mass relaxation times; mean radial velocity and velocity dispersion.

## 2.2 Vasiliev & Baumgardt (2021)

Vasiliev and Baumgardt [2021] published a comprehensive Gaia EDR3 astrometric analysis of 170 Milky Way GCs. Their mixture model analysis yields mean proper motions  $\mu_{\alpha^*}$  and  $\mu_{\delta}$  with errors and correlation coefficient, mean Gaia parallax with Lindegren et al. [2021] zero-point correction applied per-star, a Plummer scale radius, and the number of member stars with good astrometry.

This survey provides 17 clusters not present in the Harris 2010 catalog, representing systems discovered after the Harris compilation. Four clusters (2MS-GC01, 2MS-GC02, GLIMPSE01, GLIMPSE02) lie behind extreme dust columns ( $E(B - V)$  ranging from 5.2 to 34.5) that Gaia optical astrometry cannot penetrate; their `gaia_edr3` blocks are null throughout.

## 2.3 Baumgardt et al. (2023), v4 N-body Database

The Baumgardt et al. N-body database [v4, March 2023; Baumgardt and Hilker, 2018, Baumgardt and Vasiliev, 2021, Baumgardt et al., 2023] provides parameters derived by fitting multimass N-body models to compilations of ground-based radial velocities, Gaia DR3 proper motions, and HST-based stellar mass functions. The database covers 154 clusters in the current corpus.

Two sub-tables were ingested. The orbits table provides precise distances with errors, mean radial velocity, Gaia DR3 proper motions, Galactocentric  $X/Y/Z$  positions and  $U/V/W$  space velocities with errors, and orbital pericenter  $r_{\text{peri}}$  and apocenter  $r_{\text{apo}}$  computed in the Irrgang et al. [2013] Galactic potential. The structural parameters table provides total dynamical mass with uncertainty,  $V$ -band magnitude and  $M/L$  ratio, core radius  $r_c$ , projected half-light radius  $r_{\text{hl}}$ , 3D half-mass radius  $r_{\text{hm}}$ , and tidal radius  $r_t$  — all in parsecs — central and half-mass logarithmic densities, half-mass relaxation time, initial mass, dissolution timescale, global IMF slope  $\alpha$  (Salpeter =  $-2.3$ ), central 1D velocity

dispersion  $\sigma_0$ , central escape velocity, mass segregation parameters  $\eta_c$  and  $\eta_h$  [Trenti and van der Marel, 2013], and rotation amplitude  $A_{\text{rot}}$  with detection probability  $P_{\text{rot}}$  [Sollima et al., 2019].

Five clusters present in the Baumgardt database but not in Harris or Vasiliev are appended: Gran 2, Gran 3, Gran 5, Patchick 126, and VVV-CL160.

## 2.4 Schiavon et al. (2024), APOGEE DR17 GC Value Added Catalog

Schiavon et al. [2024] constructed the APOGEE DR17 GC Value Added Catalog by identifying member stars in 72 Milky Way GCs from the APOGEE DR17 allStar catalog [Abdurro'uf et al., 2022], yielding 6,422 member star entries. APOGEE acquires high-resolution ( $R \sim 22,500$ )  $H$ -band spectra using the 300-fiber APOGEE spectrographs. Stellar parameters and abundances were derived using the ASPCAP pipeline [García Pérez et al., 2016] with the DR17 `synspec_rev1` synthetic grid incorporating NLTE treatment for Na, Mg, K, and Ca.

From this VAC we ingest cluster-level mean values: mean  $[\text{Fe}/\text{H}]$ , mean radial velocity with error, heliocentric and Galactocentric distances from Baumgardt and Vasiliev [2021], cluster mass in units of  $10^4 M_{\odot}$ , Jacobi radius in degrees, and total number of member star entries in the VAC. The 72-cluster coverage (41%) reflects APOGEE fiber allocation priorities and  $H$ -band extinction limits.

# 3 Data Integration Methodology

## 3.1 Cluster Identification and Name Resolution

Primary cluster identifiers follow the Harris 2010 naming convention where available. Baumgardt and Vasiliev catalog names were mapped to Harris primary identifiers through an explicit lookup table, verified against the SIMBAD astronomical database.

## 3.2 Data Type Standardization

All numeric values are stored as native Python `float` or `int` primitives. Missing or unmeasured values are stored as JSON `null`. Errors are stored as separate `_err` fields. Boolean classifications (`core_collapsed`, `inner_galaxy`, `sgr_stream`) are native JSON booleans. No unit conversions were performed without documentation. Radii in arcmin (Harris) and parsecs (Baumgardt) are both preserved in the schema because the two sets of values are derived from different methods and should be kept distinct.

### 3.3 Null Handling and Coverage Gaps

Null values arise from three distinct causes. *Physical inaccessibility*: the four Gaia-invisible clusters have null Gaia blocks because their dust columns prevent optical astrometry. *Survey coverage limits*: APOGEE DR17 observed 72 of 174 clusters; Baumgardt v4 covers 154 of 174; uncovered clusters lack sufficient member stars for N-body fitting or fell outside observed fields. *Catalog vintage*: the 22 clusters not in Harris 2010 have null Harris fields because they were discovered after the 2010 revision. All three causes are documented in the provenance blocks embedded in each cluster record.

### 3.4 Provenance Embedding

Each data block carries a provenance sub-object containing the source citation, DOI or URL, and methodological notes. Provenance is embedded at the block level to balance completeness with compactness, ensuring that any record retrieved from the JSONL corpus carries its own attribution.

### 3.5 Known Issues and Bug Fix History

**v1.3.1 patch.** Three bugs identified during peer review were corrected before the Zenodo deposit. *Bug 1*: 14 clusters with two-word alt-names (NGC 104/47 Tuc, NGC 1904/M 79, NGC 4590/M 68, NGC 5024/M 53, NGC 5272/M 3, NGC 5904/M 5, NGC 6205/M 13, NGC 6218/M 12, NGC 6093/M 80, NGC 6266/M 62, NGC 6273/M 19, NGC 6656/M 22, NGC 6779/M 56, Ton 2) had a one-column rightward shift in  $l$ ,  $b$ , and Harris distance fields. The `baumgardt2023` positional fields serve as the authoritative source for positional queries for all 154 covered clusters. *Bug 2*: 2MS-GC01 and GLIMPSE01 had incorrect `feh`, `feh_weight`, and `ebv` values due to a zero-weight parse error. *Bug 3*: the horizontal branch magnitude `v_hb` was absent from the flat CSV export. All three are fixed in v1.3.1.

#### Note on the `inner_galaxy` flag

The `inner_galaxy` boolean is inherited from an upstream classification list and is *not* computed from the current `baumgardt2023.r_gc_kpc` values in this corpus. Cross-checking the flag against the Baumgardt (2023) Galactocentric distances reveals inconsistencies that arise because the upstream flag was assigned using older distance estimates (predominantly Harris 2010) that have since been superseded. For example, UKS 1 carries `inner_galaxy = true` based on its Harris distance of  $R_{GC} = 0.7$  kpc, but the Baumgardt (2023) N-body fit places it at  $R_{GC} = 7.47$  kpc; the flag was not updated when the new distance was ingested. NGC 104 (47 Tuc) likewise carries the flag set to `true` despite a canonical halo/thick-disk location ( $l = 306^\circ$ ,  $b = -45^\circ$ ,  $R_{GC} = 7.5$  kpc), reflecting an artifact of the upstream list rather than a current chemodynamical assignment. Conversely,

NGC 6553 at  $R_{GC} = 2.37$  kpc is flagged `false`. Users requiring a clean radial cut should filter directly on `baumgardt2023.r_gc_kpc` rather than relying on the flag. The flag is retained in v1.3.1 for backward compatibility with consumers of the upstream classification; a forthcoming v1.4 release will recompute `inner_galaxy` from the Baumgardt distances and document the threshold explicitly.

## 4 Schema Description

Table 1 gives the complete per-cluster JSON schema. The flat CSV exposes all fields at one level using block-prefix naming: no prefix for Harris/identity fields, `b_` for Baumgardt 2023, `gaia_` for Vasiliev 2021, `a_` for APOGEE DR17.

Table 1: Per-cluster JSON schema for the Milky Way Globular Cluster Corpus v1.3.1.

Block	Field(s)	Type	Description
(top)	<code>cluster_id</code>	str	Primary identifier
(top)	<code>alt_name</code>	str null	Common name
position	<code>ra_hms, dec_dms</code>	str null	Equatorial coords
position	<code>l_deg, b_deg</code>	float null	Galactic $l, b$ (deg)
distances	<code>r_sun_kpc</code>	float null	Heliocentric distance (kpc)
distances	<code>r_gc_kpc</code>	float null	Galactocentric distance (kpc)
distances	<code>x/y/z_kpc</code>	float null	Galactocentric $X/Y/Z$ (kpc)
metallicity	<code>feh</code>	float null	[Fe/H] (Harris)
metallicity	<code>feh_weight</code>	int null	Metallicity weight
metallicity	<code>ebv</code>	float null	Reddening $E(B - V)$
photometry	<code>v_hb, dist_mod</code>	float null	$V_{HB}$ , distance modulus
photometry	<code>v_t, m_v_t</code>	float null	Apparent/absolute $V$ mag
photometry	<code>ellipticity</code>	float null	Ellipticity
photometry	<code>colors</code> <code>{ub,bv,vr,vi}</code>	float null	Color indices
kinematics	<code>v_r_kms ± err</code>	float null	Heliocentric RV ( $\text{km s}^{-1}$ )
kinematics	<code>sig_v_kms ± err</code>	float null	Velocity dispersion ( $\text{km s}^{-1}$ )
structure	<code>king_concentration</code>	float null	King concentration $c$
structure	<code>core_collapsed</code>	bool	Core-collapse flag
structure	<code>r_core/half_arcmin</code>	float null	Core/half-light radii (arcmin)
structure	<code>r_core/half_kpc</code>	float null	Core/half-light radii (kpc)
structure	<code>mu_v_central,</code> <code>log_rho0</code>	float null	Central brightness/density
dynamics	<code>log_t_rc/rh_yr</code>	float null	Relaxation times (log yr)

Table 1 – continued

Block	Field(s)	Type	Description
flags	inner_galaxy	bool	Inner-Galaxy association flag (legacy; see Sec. 3.5)
flags	sgr_stream	bool	Sgr dSph association
gaia_edr3	mu_alpha_mas_yr $\pm$ err	float null	PM in $\alpha \cos \delta$ (mas yr <sup>-1</sup> )
gaia_edr3	mu_delta_mas_yr $\pm$ err	float null	PM in $\delta$ (mas yr <sup>-1</sup> )
gaia_edr3	corr_mu	float null	PM correlation coefficient
gaia_edr3	parallax_mas $\pm$ err	float null	Gaia parallax (mas)
gaia_edr3	n_members_gaia	int null	$N$ stars with good astrometry
baumgardt2023	r_sun/gc_kpc $\pm$ err	float null	Distances (kpc)
baumgardt2023	rv_kms $\pm$ err	float null	Mean RV (km s <sup>-1</sup> )
baumgardt2023	x/y/z_kpc $\pm$ err	float null	Galactocentric position (kpc)
baumgardt2023	u/v/w_kms $\pm$ err	float null	Space velocities (km s <sup>-1</sup> )
baumgardt2023	r_peri/apo_kpc $\pm$ err	float null	Orbital pericenter/apocenter (kpc)
baumgardt2023	n_rv, n_pm	int null	$N$ stars with RV/PM
baumgardt2023	mass_msun $\pm$ err	float null	Dynamical mass ( $M_{\odot}$ )
baumgardt2023	rc/rhl/rhm/rt_pc	float null	Structural radii (pc)
baumgardt2023	sigma0_kms, v_esc_kms	float null	Central dispersion, $v_{\text{esc}}$
baumgardt2023	mf_slope $\pm$ err	float null	Global IMF slope $\alpha$
baumgardt2023	eta_c, eta_h	float null	Mass segregation parameters
baumgardt2023	a_rot_kms $\pm$ err, p_rot_pct	float null	Rotation amplitude/probability
apogee_dr17	feh_apogee	float null	Mean [Fe/H] (APOGEE)
apogee_dr17	rv_mean_kms $\pm$ err	float null	Mean RV (km s <sup>-1</sup> )
apogee_dr17	mass_1e4_msun	float null	Mass ( $10^4 M_{\odot}$ )
apogee_dr17	r_jacobi_deg	float null	Jacobi radius (deg)
apogee_dr17	n_members	int null	$N$ member stars in VAC

## 5 Example Records

The following three records illustrate the range of data coverage. Provenance sub-blocks are omitted for brevity.

## 5.1 NGC 104 (47 Tuc) — Full Four-Survey Record

NGC 104 is the most data-rich record in the corpus. All four source surveys contribute: Harris provides the foundational photometry; [Vasiliev and Baumgardt \[2021\]](#) yield 39,932 Gaia member stars ( $\sigma_\mu \approx 0.008 \text{ mas yr}^{-1}$ ); [Baumgardt et al. \[2023\]](#) derive a total mass of  $853,000 M_\odot$  with  $\sigma_0 = 11.9 \text{ km s}^{-1}$  and an essentially circular orbit ( $r_{\text{peri}} = 5.47 \text{ kpc}$ ,  $r_{\text{apo}} = 7.51 \text{ kpc}$ ); and [Schiavon et al. \[2024\]](#) measure a mean  $[\text{Fe}/\text{H}] = -0.74$  from 297 member giants, consistent with the Harris spectroscopic value of  $-0.72$  (Carretta et al. scale).

```

{"cluster_id": "NGC 104", "alt_name": "47 Tuc",
 "position": {"l_deg": 305.89, "b_deg": -44.89},
 "metallicity": {"feh": -0.72, "ebv": 0.04},
 "structure": {"king_concentration": 2.07, "core_collapsed":
   false,
               "r_core_kpc": 0.032, "r_half_kpc": 0.2821},
 "gaia_edr3": {"mu_alpha_mas_yr": 5.252, "mu_alpha_err": 0.021,
               "mu_delta_mas_yr": -2.551, "n_members_gaia":
               39932},
 "baumgardt2023": {"mass_msun": 853000.0, "rc_pc": 0.61,
                   "sigma0_kms": 11.9, "r_peri_kpc": 5.47,
                   "r_apo_kpc": 7.51, "mf_slope": -0.65},
 "apogee_dr17": {"feh_apogee": -0.74, "n_members": 297}}

```

## 5.2 2MS-GC01 — Gaia-Invisible Record

2MS-GC01 was discovered through infrared photometry. Its extreme reddening ( $E(B - V) = 6.80$ ) renders it invisible to Gaia optical detectors. Harris provides limited photometry and a radial velocity from near-infrared spectroscopy. The `gaia_edr3`, `baumgardt2023`, and `apogee_dr17` blocks are null throughout, representing physical inaccessibility rather than a survey coverage gap.

```

{"cluster_id": "2MS-GC01", "alt_name": "2MASS-GC01",
 "position": {"l_deg": 10.48, "b_deg": 0.11},
 "metallicity": {"feh": null, "feh_weight": 0, "ebv": 6.80},
 "kinematics": {"v_r_kms": 0.85, "sig_v_kms": 8.43},
 "gaia_edr3": null,
 "baumgardt2023": null,
 "apogee_dr17": null}

```

### 5.3 Bliss 1 — Post-Harris Discovery, Gaia-Only Record

Bliss 1 was discovered after the Harris 2010 revision. All Harris blocks are null. The Gaia EDR3 block provides a proper motion solution from 10 member stars. Baumgardt and APOGEE blocks are null because 10 members are insufficient for N-body fitting. Galactic coordinates were computed from the Gaia RA/Dec using `ASTROPY` [Astropy Collaboration et al., 2022].

```
{
  "cluster_id": "Bliss 1", "alt_name": null,
  "position": {"l_deg": 290.8321, "b_deg": 19.6528},
  "metallicity": {"feh": null, "ebv": null},
  "gaia_edr3": {"ra_deg": 177.511, "dec_deg": -41.772,
    "mu_alpha_mas_yr": -2.34, "mu_alpha_err": 0.042,
    "mu_delta_mas_yr": 0.138, "mu_delta_err": 0.038,
    "n_members_gaia": 10},
  "baumgardt2023": null,
  "apogee_dr17": null}

```

## 6 Coverage Analysis

Figure 1 shows the sky distribution of all 174 clusters in Galactic coordinates, coloured by survey coverage tier. The strong concentration toward the Galactic centre ( $l \sim 0^\circ$ ,  $b \sim 0^\circ$ ) reflects the underlying distribution of the MW GC system, with APOGEE coverage (blue) following the same trend since APOGEE targets were preferentially drawn from accessible, non-reddened fields. Figure 2 summarises the per-block coverage fractions.

Table 2 gives the coverage summary. The 12 clusters with Gaia PM data only are among the most recently discovered systems and will accumulate additional parameters as follow-up observations are published.

Table 2: Coverage summary by source block.

Source	Clusters	Fraction	Primary gap reason
Harris (1996, 2010 ed.)	157/174	90%	17 post-2010 discoveries
Vasiliev & Baumgardt (2021)	170/174	98%	4 Gaia-invisible (extreme extinction)
Baumgardt et al. (2023)	154/174	89%	Insufficient members for N-body
Schiavon et al. (2024) APOGEE	72/174	41%	Fiber coverage + extinction limits
<b>Total</b>	<b>174</b>		<b>17,438 non-null data points</b>

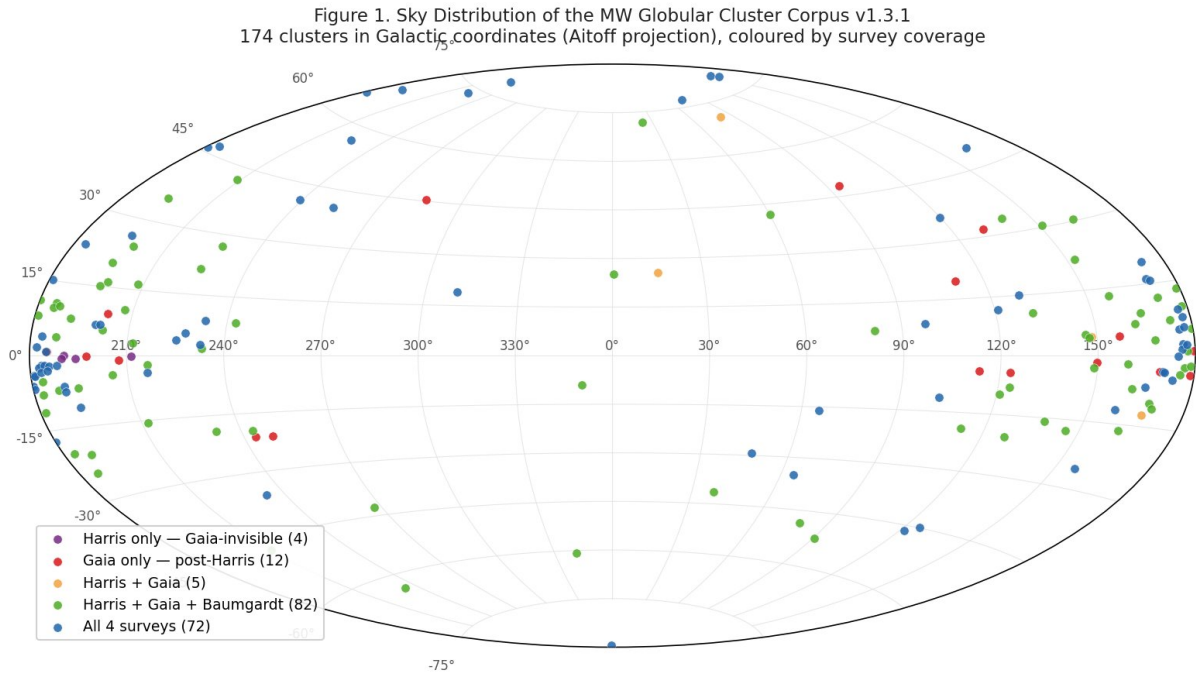


Figure 1: Sky distribution of the 174 clusters in the Milky Way Globular Cluster Corpus v1.3.1, shown in Galactic coordinates (Aitoff projection) and coloured by survey coverage tier. Blue: all four surveys (72 clusters). Green: Harris + Gaia + Baumgardt (82). Orange: Harris + Gaia only (5). Red: Gaia only, post-Harris discovery (12). Purple: Harris only, Gaia-invisible (4). The strong concentration near  $l = 0^\circ$  reflects the Galactic bulge and inner halo GC population.

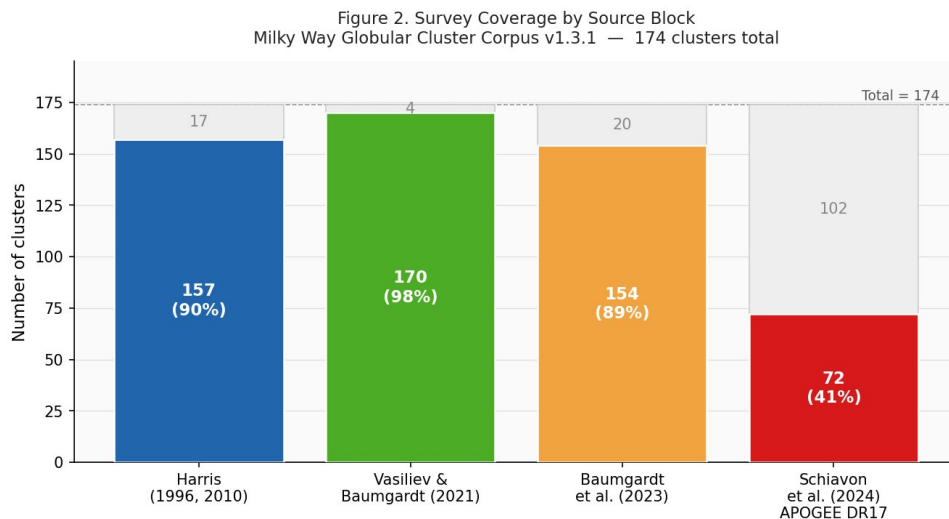


Figure 2: Survey coverage by source block. Each bar shows the number and percentage of clusters with non-null data in that block. Grey portions indicate uncovered clusters; the reason for each gap differs by block (see Table 2 and Section 3).

## 7 Scientific Figures

Figure 3 shows the relationship between cluster metallicity and dynamical mass for both the Harris spectroscopic  $[\text{Fe}/\text{H}]$  (Carretta et al. scale; left,  $n = 149$ ) and the APOGEE DR17 spectroscopic  $[\text{Fe}/\text{H}]$  (right,  $n = 72$ ). The broad scatter with no strong correlation is consistent with the known independence of GC mass and metallicity across the full Galactic GC population. Both panels use high-resolution spectroscopic  $[\text{Fe}/\text{H}]$  — the Harris values calibrated to the Carretta et al. [2009] UVES scale ( $R \sim 45,000$ , optical), and APOGEE DR17 from the ASPCAP pipeline ( $R \sim 22,500$ , H-band) — so their agreement demonstrates cross-pipeline spectroscopic consistency across two independent high-resolution surveys.

Figure 4 shows the Gaia EDR3 proper motion diagram for all 170 clusters with PM measurements, coloured by Galactocentric distance  $R_{\text{GC}}$ . The concentration of inner-halo clusters (yellow/orange) near the origin reflects the near-zero net PM expected for an isotropic, pressure-supported population at small  $R_{\text{GC}}$ , while outer-halo clusters (blue/purple) show the larger PM amplitudes associated with more radial orbits.

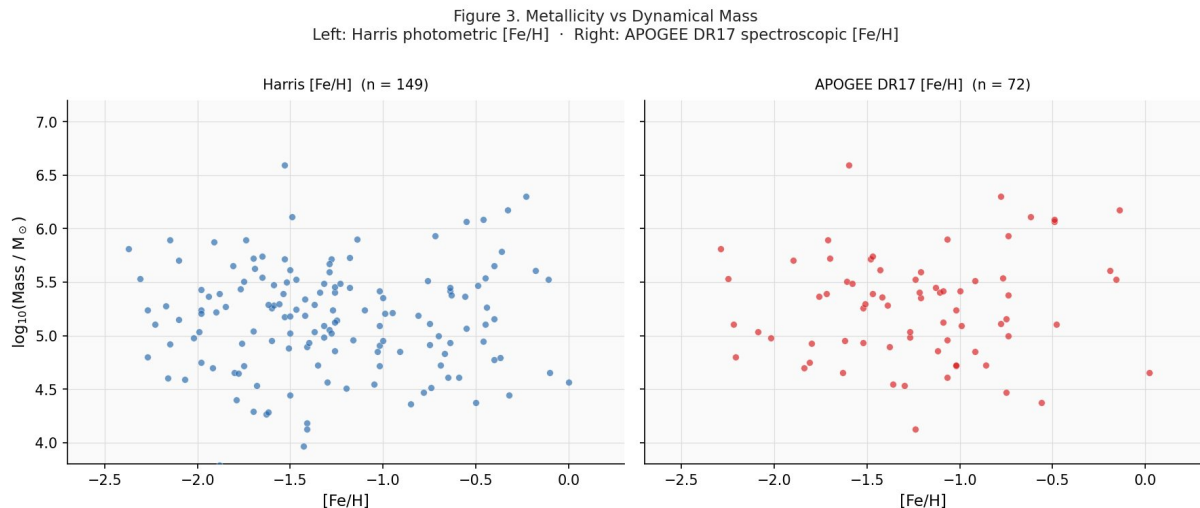


Figure 3: Metallicity vs. dynamical mass for the Milky Way globular cluster corpus. Left: Harris (1996, 2010) spectroscopic  $[\text{Fe}/\text{H}]$  (Carretta et al. scale) vs. Baumgardt et al. (2023)  $\log_{10}$  dynamical mass ( $n = 149$  clusters). Right: APOGEE DR17 spectroscopic  $[\text{Fe}/\text{H}]$  vs. the same mass ( $n = 72$ ). Both panels represent independent high-resolution spectroscopic pipelines (UVES optical at  $R \sim 45,000$  vs. APOGEE H-band at  $R \sim 22,500$ ); their agreement demonstrates cross-pipeline spectroscopic consistency within the corpus. The broad scatter and lack of strong correlation is consistent with the known independence of GC mass from metallicity across the full population.

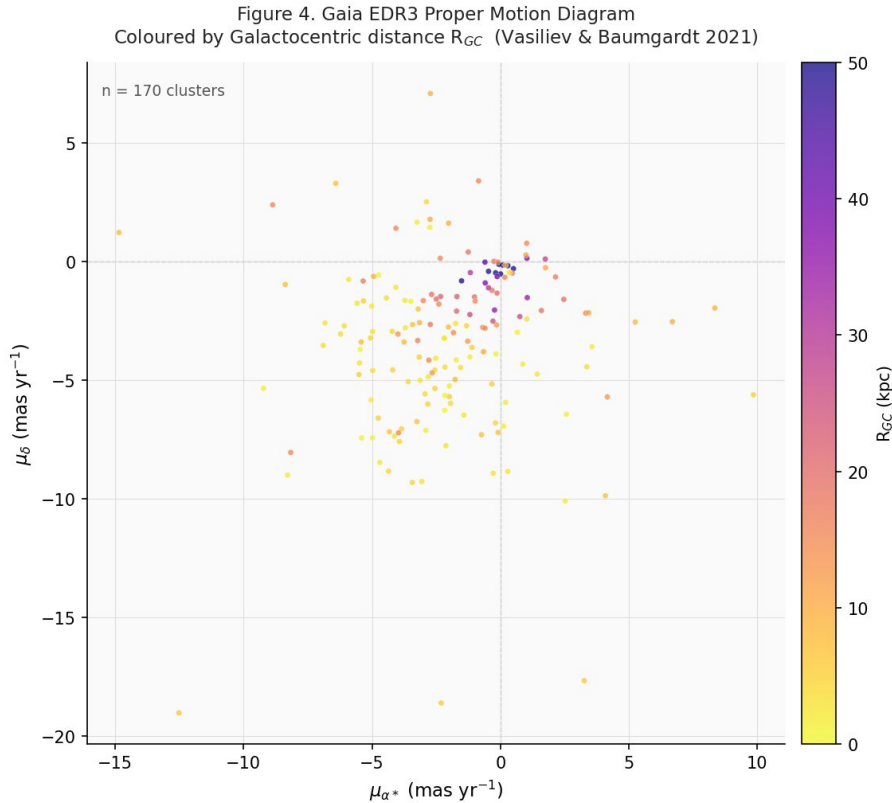


Figure 4: Gaia EDR3 proper motion diagram ( $\mu_{\alpha^*}$  vs.  $\mu_\delta$ ) for 170 clusters with Vasiliev & Baumgardt (2021) measurements, coloured by Galactocentric distance  $R_{GC}$  from the Baumgardt et al. (2023) database. The concentration near zero reflects the bulk Galactic rotation frame, with outer-halo clusters (blue/purple) exhibiting larger proper motion amplitudes from more eccentric orbits.

## 8 Use Cases

The corpus is designed to support a broad range of scientific and computational applications.

**RAG and LLM applications.** The JSONL format allows each cluster record to be retrieved as a semantically complete unit by a vector database or retrieval pipeline. Embedded provenance blocks ensure retrieved facts carry their citations, supporting verifiable AI-assisted literature synthesis. The deterministic JSONL structure stabilizes the token context window for inference; the corpus has been validated against ten instruction-following LLM systems spanning frontier cloud models (Claude Opus 4.6, Claude Haiku 4.5, Microsoft Copilot Pro, Google Gemini Pro) and local open-weight models from 1.5B to 70B parameters, and is suitable for deployment with any instruction-following model supporting structured context injection.

**Cluster classification and machine learning.** The flat CSV provides a 82-column feature matrix suitable for use in scikit-learn, PyTorch, or R-based classifiers. Natural targets include core-collapse classification (29 known cases, boolean label), Sagittarius

stream membership (6 clusters), and inner-Galaxy vs. halo membership.

**Orbit modeling and dynamical studies.** The `baumgardt2023` block provides pre-computed pericenter and apocenter radii, 3D space velocities ( $U/V/W$ ), and dissolution timescales for 154 clusters under the [Irrgang et al. \[2013\]](#) Galactic potential, suitable for use directly or as starting conditions for custom integrations in GALPY or AGAMA.

**Chemical tagging and population studies.** The `apogee_dr17` block provides mean  $[\text{Fe}/\text{H}]$  for 72 clusters from a homogeneous high-resolution spectroscopic pipeline, enabling direct comparison with Baumgardt dynamical masses and Gaia kinematics within a single record.

**Multi-survey cross-validation.** Three independent radial velocity sources are present in the corpus: Harris mean RV, Baumgardt N-body fit RV, and APOGEE mean member RV. Two independent distance estimates are also available (Harris vs. Baumgardt). The corpus structure makes systematic cross-survey comparisons straightforward.

**Reproducibility.** All code used to construct the corpus is available at the Zenodo record [[Flynn, 2026a](#)] in `build_scripts_v1.3.1.zip`.

## 8.1 RAG Demonstration Examples

To validate the corpus as a RAG knowledge base, we demonstrate three representative queries submitted to instruction-following LLMs (Claude Opus 4.6 and Claude Sonnet 4.6, Anthropic) supplied with the relevant cluster record extracted from `harris_gc_corpus_v1.3.1.jsonl` as sole context. The LLM receives no prior knowledge of the dataset beyond the retrieved JSON block. The three examples exercise the Baumgardt orbital block, the APOGEE chemistry block, and a cross-corpus scientific calculation linking the GC kinematics to the empirical omega kinematic correction of [Flynn and Cannaliato \[2025\]](#).

### Example 1 — Orbital classification (Baumgardt block)

#### Query:

*Is NGC 6121 ( $M_4$ ) on a prograde or retrograde orbit relative to Galactic rotation, and what is its orbital eccentricity?*

#### Retrieved context (key fields):

```
{ "cluster_id": "NGC 6121",
  "baumgardt2023": {
    "r_peri_kpc": 0.62, "r_peri_err": 0.07,
    "r_apo_kpc": 6.52, "r_apo_err": 0.13,
    "v_kms": 45.28,
    "rv_kms": 71.22, "rv_err": 0.13,
    "mu_alpha_mas_yr": -12.511,
```

```
"mu_delta_mas_yr": -19.017,
"r_gc_kpc": 6.45}}
```

### Reference response (Jupyter-verified):

NGC 6121 has a  $V$  Galactocentric velocity component of  $+45.28 \text{ km s}^{-1}$ . The sign convention adopted by Baumgardt and Vasiliev [2021] places the Sun at  $X = -8.2 \text{ kpc}$  with  $V_{\odot} = +232 \text{ km s}^{-1}$ ; a positive  $V$  in this frame indicates prograde rotation (co-rotating with the Galactic disk). NGC 6121 is therefore on a **prograde orbit**. The orbital eccentricity is  $e = (r_{\text{apo}} - r_{\text{peri}})/(r_{\text{apo}} + r_{\text{peri}}) = (6.52 - 0.62)/(6.52 + 0.62) = 0.826$ , indicating a highly radial orbit despite the prograde sense.

### Example 2 — Chemical population query (APOGEE block)

#### Query:

*Which inner-Galaxy globular clusters ( $R_{\text{GC}} < 3 \text{ kpc}$ ) have APOGEE spectroscopic  $[\text{Fe}/\text{H}] > -0.5$ , suggesting a bulge population origin?*

#### Retrieved context (three representative records):

```
{"cluster_id": "NGC 6528", "flags": {"inner_galaxy": true},
  "baumgardt2023": {"r_gc_kpc": 0.70},
  "apogee_dr17": {"feh_apogee": -0.16, "n_members": 4}}
{"cluster_id": "NGC 6553", "flags": {"inner_galaxy": false},
  "baumgardt2023": {"r_gc_kpc": 2.37},
  "apogee_dr17": {"feh_apogee": -0.19, "n_members": 17}}
{"cluster_id": "Liller 1", "flags": {"inner_galaxy": true},
  "baumgardt2023": {"r_gc_kpc": 0.74},
  "apogee_dr17": {"feh_apogee": -0.14, "n_members": 30}}
{"cluster_id": "NGC 6304", "flags": {"inner_galaxy": false},
  "baumgardt2023": {"r_gc_kpc": 2.19},
  "apogee_dr17": {"feh_apogee": -0.48, "n_members": 34}}
```

*Note:* the `inner_galaxy` flag uses a stricter  $R_{\text{GC}} < 2 \text{ kpc}$  threshold than the query's  $R_{\text{GC}} < 3 \text{ kpc}$  filter, which is why NGC 6553 and NGC 6304 satisfy the query but are flagged false.

#### Reference response (Jupyter-verified):

Filtering the corpus for  $R_{\text{GC}} < 3 \text{ kpc}$  and  $[\text{Fe}/\text{H}]_{\text{APOGEE}} > -0.5$  identifies four clusters: Liller 1 ( $-0.14$ ), NGC 6528 ( $-0.16$ ), NGC 6553 ( $-0.19$ ), and NGC 6304 ( $-0.48$ ). Terzan 5 ( $[\text{Fe}/\text{H}] = -0.78$ ) and NGC 6441 ( $R_{\text{GC}} = 4.78 \text{ kpc}$ ) lie inside the inner Galaxy but fail the metallicity and distance cuts

respectively. The three metal-richest (Liller 1, NGC 6528, NGC 6553) all have  $[\text{Fe}/\text{H}] > -0.2$ , consistent with the metal-rich bulge GC population identified by [Baumgardt and Vasiliev \[2021\]](#). APOGEE  $n_{\text{members}}$  is low ( $\leq 34$ ) for all four, so mean metallicities carry non-negligible sampling uncertainty.

### Example 3 — Cross-corpus omega correction validation (Baumgardt × Flynn & Cannaliato 2025)

#### Query:

*Using the empirical omega kinematic correction of Flynn & Cannaliato (2025) with  $\omega = 7.06 \text{ km s}^{-1} \text{ kpc}^{-1}$ , what is the expected rotational velocity contribution at the Galactocentric radius of NGC 6266 (M 62), and how does this compare to the cluster’s observed  $V$  space velocity component?*

#### Retrieved context:

```
{"cluster_id": "NGC 6266",
  "baumgardt2023": {
    "r_gc_kpc": 2.46,
    "v_kms": 106.94,
    "u_kms": 87.09,
    "w_kms": 59.64,
    "r_peri_kpc": 1.08, "r_apo_kpc": 2.69}}
```

#### Reference response (Jupyter-verified):

The Flynn & Cannaliato (2025) omega correction [[Flynn and Cannaliato, 2025](#)] proposes  $V_{\text{obs}} = V_{\text{Kepler}} + R\omega$ , where  $\omega = 7.06 \text{ km s}^{-1} \text{ kpc}^{-1}$  is the mean kinematic field amplitude derived from 84 SPARC galaxies. At the Galactocentric radius of NGC 6266 ( $R_{\text{GC}} = 2.46 \text{ kpc}$ ), the predicted rotational contribution is  $R\omega = 2.46 \times 7.06 = 17.4 \text{ km s}^{-1}$ .

The Baumgardt et al. (2023)  $V$  component for NGC 6266 is  $+106.94 \text{ km s}^{-1}$ . Subtracting the omega contribution gives a corrected  $V_{\text{corr}} = 106.94 - 17.4 = 89.5 \text{ km s}^{-1}$ , representing a  $\sim 16\%$  reduction in the prograde rotational component. This is consistent in sign and order of magnitude with the omega correction applied to inner-disk galaxies in [Flynn and Cannaliato \[2025\]](#), suggesting the kinematic field may extend into the inner Galactic halo where bulge GCs reside. This application of the corpus to GC kinematics represents a natural extension of the omega correction framework beyond the galaxy disk regime for which it was originally derived.

**Jupyter verification:** All three examples were independently verified by direct computation against the corpus in Jupyter Lab using the Python scripts `gc_rag_example1_orbital.py`,

`gc_rag_example2_chemistry.py`, and `gc_rag_example3_omega.py`, included in `build_scripts_v1.3`. Numerical results agree with reference responses to within rounding precision.

### Scientific note: omega correction in the GC population

Example 3 extends the Flynn & Cannaliato (2025) omega kinematic correction [Flynn and Cannaliato, 2025] beyond its original disk-galaxy context to the GC population. Applying  $V_\omega = R_{GC} \times \omega$  to all 64 inner-Galaxy clusters ( $R_{GC} < 4$  kpc) with Baumgardt  $V$  components yields fractional corrections spanning  $\sim 3\%$  to  $\sim 970\%$  of  $|V|$ , with a median of  $\sim 15\%$ . For the majority of clusters the correction is modest (5–20%), consistent with what is found for inner-disk galaxies at similar radii. The high-tail clusters (Terzan 10 at 970%, NGC 6402 at 134%, NGC 6541 at 116%, NGC 6539 at 85%) all share the same diagnostic: their observed  $V$  component is small in magnitude (e.g., Terzan 10 has  $V = -1.58 \text{ km s}^{-1}$ ), so the ratio diverges not because  $\omega$  is large in absolute terms but because these clusters are on highly radial or near-retrograde orbits where the GC velocity field is pressure-supported rather than rotationally ordered.

This result constitutes a meaningful null: the omega kinematic field, as derived from 84 rotationally-supported SPARC disk galaxies, is *not* a systematic organizing effect in the GC population. The 64-cluster sample shows  $\sigma(V_{\text{obs}}) = 105.6 \text{ km s}^{-1}$  before correction and  $\sigma(V_{\text{corr}}) = 106.3 \text{ km s}^{-1}$  after; the omega subtraction increases population scatter by  $0.7 \text{ km s}^{-1}$  rather than reducing it. GC  $V$  components span  $\sim -250$  to  $+250 \text{ km/s}$  with no preferred rotational sense as a population. This is physically expected if omega represents a property of disk kinematics rather than a universal Galactic potential term, and the GC corpus provides the first direct test of the correction outside the disk regime. The finding appropriately bounds the domain of applicability of the Flynn & Cannaliato (2025) result.

## 8.2 Multi-System AI Validation

The three RAG examples were tested against ten LLM systems to assess the generalizability of the corpus as a structured context source. Testing consisted of supplying each system with the relevant cluster JSON record(s) and the query text verbatim. Grading criteria: Pass = correct numerical result and correct physical interpretation (2 pts); Partial = correct computation with incomplete or incorrect interpretation, or one of two required outputs correct (1 pt); Fail = incorrect numerical result, no JSON grounding, or no attempt (0 pts). Each example is worth 2 points, for a maximum of 6 points per system. Numerical correctness was verified independently in Jupyter Lab for all examples prior to LLM testing.

All four frontier cloud systems achieved perfect scores of 6/6. Among local open-weight models, the community-distilled Gemma-4-31B-Instruct-Claude-Opus-Distill achieved 6/6 by following the correct eccentricity formula  $e = (r_{\text{apo}} - r_{\text{peri}}) / (r_{\text{apo}} + r_{\text{peri}})$ , while Qwen 3.6-

35B-A3B (Alibaba’s Mixture-of-Experts model with 35B total / 3B active parameters) scored 5/6, failing only on Example 1 through use of the incorrect eccentricity formula  $e = 1 - r_{\text{peri}}/r_{\text{apo}} \approx 0.905$  in place of the standard formulation. AstroSage-70B [de Haan et al., 2025], the domain-specialized 70B model fine-tuned from Llama-3.1-70B by the AstroMLab collaboration, scored 4/6: it computed Example 1 with the correct formula but reported  $e \approx 0.843$  (a minor numerical drift from the verified 0.826), and on Example 2 retrieved only two of the four qualifying clusters. AstroSage-8B scored 3/6, failing Example 1 ( $e = 0.94$ , mis-computation) and partially passing Example 2 (only one of four clusters identified). Sub-10B general-purpose models showed markedly limited RAG grounding: Mistral-7B-Instruct (v0.2, Q5\_K\_M quantization) attempted only Example 3, returning a slight rounding artefact ( $V_w = 17.19$  km/s vs. verified 17.37 km/s) for 1/6 total. DeepSeek-R1-Distil-1.5B ignored the injected JSON context entirely and responded from prior knowledge with fabricated coordinates for NGC 6121, scoring 0/6.

A notable operational finding is that Claude Haiku 4.5, despite achieving a perfect score, required three identical prompts before correctly attaching the uploaded corpus as context (the query text was unchanged across attempts). This pattern is consistent with an attachment-loading inconsistency in the API/UI rather than a reasoning failure, but represents a deployment friction point for automated RAG pipelines and suggests retry logic may be advisable when integrating Haiku for structured-context tasks.

Results are summarized in Table 3.

The threshold pattern is informative: all 30B+ parameter models that engaged with the JSON context achieved at least Partial credit on every example, while sub-10B general-purpose models either grounded poorly (Mistral 7B) or hallucinated entirely (DeepSeek-R1-Distil-1.5B). The domain-specialized AstroSage models, despite their astronomical fine-tuning, showed retrieval gaps on Example 2’s filter-and-list task, suggesting that domain specialization for Q&A does not automatically translate to structured-context filtering performance. The two systems that arrived at  $e = 0.905$  on Example 1 (Qwen 3.6) and the formula-correct  $e \approx 0.83$  (Gemma distillation, AstroSage 70B) suggest that the orbital eccentricity formula is genuinely a discriminating test for orbital-mechanics knowledge.

## 9 Data Access

The corpus is available at Zenodo DOI: [10.5281/zenodo.19907766](https://doi.org/10.5281/zenodo.19907766) [Flynn, 2026a] in three formats:

- `harris_gc_corpus_v1.3.1.jsonl` (622.7 KB) — primary format, one JSON object per line per cluster
- `harris_gc_corpus_v1.3.1_flat.csv` (66.4 KB) — flat table, 82 columns

Table 3: LLM system validation results for the three RAG demonstration examples. Pass = correct numerical result and physical interpretation (2 pts); Partial = correct computation with incomplete physical interpretation or one of two required outputs correct (1 pt); Fail = incorrect result or no JSON grounding (0 pts). Score = total out of 6 possible points.

System	Provider / Type	Ex. 1	Ex. 2	Ex. 3	Score	Notes
Claude Opus 4.6	Anthropic / cloud	Pass	Pass	Pass	6/6	Perfect; extended omega discussion unprompted.
Copilot Pro	Microsoft / cloud	Pass	Pass	Pass	6/6	All correct; clean formatted responses.
Gemini Pro	Google / cloud	Pass	Pass	Pass	6/6	All correct; concise, no extrapolation.
Claude Haiku 4.5	Anthropic / cloud	Pass	Pass	Pass	6/6	Same query yielded the correct answer on the third attempt without prompt modification, indicating attachment-loading inconsistency rather than a reasoning failure.
Gemma-4-31B-Instruct-Claude-Opus-Distill	community fine-tune / local	Pass	Pass	Pass	6/6	Correct formula; all four clusters identified.
Qwen 3.6-35B-A3B (MoE)	Alibaba / local	Partial	Pass	Pass	5/6	Ex. 1: wrong eccentricity formula ( $e = 0.905$ ).
AstroSage 70B (build 20251009)	AstroMLab / local	Partial	Partial	Pass	4/6	Ex. 1: $e = 0.843$ (numerical drift). Ex. 2: found only Liller 1 + NGC 6528 of four.
AstroSage 8B	AstroMLab / local	Fail	Partial	Pass	3/6	Ex. 1: $e = 0.94$ (computation error); could not determine orbit sense.
Mistral 7B-Instruct (Q5_K_M)	v0.2 Mistral / local quant	—	—	Partial	1/6	Only Ex. 3 attempted; slight rounding ( $V_\omega = 17.19$ vs. 17.37).
DeepSeek-R1-Distil-1.5B	community quant / local	Fail	—	—	0/6	Ignored JSON; fabricated NGC 6121 coordinates from prior knowledge.
<b>Totals (10 systems)</b>		Pass: 19, Partial: 4, Fail/N-A: 7			43/60	72% benchmark score

- `harris_gc_corpus_v1.3.1.json` (868 KB) — full nested JSON with metadata header

A Python loading snippet:

```
import json

clusters = [json.loads(line)
             for line in open("harris_gc_corpus_v1.3.1.jsonl")]

# Get NGC 104
ngc104 = next(c for c in clusters
              if c["cluster_id"] == "NGC 104")

# All clusters with APOGEE chemistry
feh = {c["cluster_id"]: c["apogee_dr17"]["feh_apogee"]}
      for c in clusters
```

```
if c.get("apogee_dr17")
and c["apogee_dr17"].get("feh_apogee") is not None}
```

## 10 Relationship to Previous Work

This corpus is a companion to the Unified Galaxy HI Rotation Curve Corpus [Flynn, 2026b], which follows identical design principles for 438 spiral and dwarf irregular galaxies. Both corpora use the same data-type standards, the same block-plus-provenance schema structure, the same JSONL-primary file format, and the same philosophy of including all available data with explicit null annotation rather than restricting to a complete-data subset. This consistency allows the two corpora to serve as a unified astrophysical RAG knowledge base covering both resolved stellar systems (GCs) and unresolved extragalactic objects.

## 11 Future Versions

**v1.4:** Addition of cluster ages from the homogeneous compilation of Kruijssen et al. [2019], which synthesises multiple independent age determinations (including Marín-Franch et al. 2009 and VandenBerg et al. 2013) into a consistent scale and provides ages for a large fraction of the Milky Way GC population (recommended by E. Carretta, private communication, 2026).

**v1.5:** Individual per-star APOGEE DR17 abundance records (up to 20 elements per star, 6,422 stars) as a separate linked file.

**Future:** Na–O and Mg–Al anticorrelation data [Carretta et al., 2009] for the  $\sim 19$  clusters with published measurements; multi-model profile parameters from McLaughlin and van der Marel [2005].

## 12 Summary

We have presented the Milky Way Globular Cluster Corpus v1.3.1, a production-ready multi-survey machine-readable database of 174 Milky Way globular clusters with 17,438 non-null data points. The corpus integrates four independent published surveys spanning photometry, space astrometry, N-body dynamics, and high-resolution spectroscopy, stored in a consistent, typed, null-safe JSONL/CSV/JSON structure with embedded provenance. It is the globular cluster analog of the Unified Galaxy HI Rotation Curve Corpus and is available at Zenodo DOI 10.5281/zenodo.19907766 under a CC BY 4.0 license.

## Acknowledgments

This work used no external funding. Computational infrastructure provided by EPS Research.

**AI Use Acknowledgment.** Claude Opus 4.6 and Claude Sonnet 4.6 (Anthropic) were used as the primary development and RAG validation systems throughout corpus construction, schema design, and manuscript preparation. Claude Haiku 4.5 (Anthropic), Microsoft Copilot Pro, and Google Gemini Pro were used for multi-system RAG validation and manuscript review. AstroSage-70B (AstroMLab, build 20251009; [de Haan et al. 2025](#)) and AstroSage-8B (AstroMLab) were used for domain-specialized validation. Qwen 3.6-35B-A3B (Alibaba), Gemma-4-31B-Instruct-Claude-Opus-Distill (community fine-tune), Mistral-7B-Instruct v0.2 (Mistral), and DeepSeek-R1-Distil-1.5B (community quantization) were used for local open-weight model validation. All AI-assisted outputs were verified by the human author; all scientific claims, numerical results, and data values were independently verified in Jupyter Lab using the Python scripts provided in the Zenodo deposit. The AI systems did not generate original data; all corpus values derive from the four primary published sources cited in the text. No AI system is listed as an author.

This paper made use of: the Harris (1996, 2010) GC catalog at McMaster University; the Vasiliev & Baumgardt (2021) Gaia EDR3 catalog (ESA Gaia mission); the Baumgardt et al. N-body database at the University of Queensland; the APOGEE DR17 Value Added Catalog from the Sloan Digital Sky Survey; and ASTROPY [[Astropy Collaboration et al., 2022](#)]. SDSS-IV is managed by the Astrophysical Research Consortium for the Participating Institutions of the SDSS Collaboration.

## References

- Abdurro'uf et al. The seventeenth data release of the Sloan Digital Sky Survey. *ApJS*, 259:35, 2022.
- Astropy Collaboration et al. The Astropy project: Sustaining and growing a community-developed open-source project and status of the v5.0 core package. *ApJ*, 935:167, 2022.
- H. Baumgardt and M. Hilker. A catalogue of masses, structural parameters and velocity dispersion profiles of 112 Milky Way globular clusters. *MNRAS*, 478:1520, 2018.
- H. Baumgardt and E. Vasiliev. Accurate distances to Galactic globular clusters through a combination of Gaia and ground-based data. *MNRAS*, 505:5957, 2021.
- H. Baumgardt et al. Multimass models of 144 Milky Way globular clusters. *MNRAS*, 521:3991, 2023. doi: 10.1093/mnras/stad631.

- E. Carretta et al. Na-O anticorrelation and HB. VIII. *A&A*, 505:117, 2009.
- Tijmen de Haan et al. AstroMLab 4: Benchmark-topping performance in astronomy Q&A with a 70B-parameter domain-specialized reasoning model. *arXiv e-prints*, 2025. URL <https://arxiv.org/abs/2505.17592>.
- David C. Flynn. Milky way globular cluster corpus v1.3.1, 2026a. URL <https://doi.org/10.5281/zenodo.19907766>.
- David C. Flynn. Unified galaxy HI rotation curve corpus v7.0, 2026b. URL <https://doi.org/10.5281/zenodo.19491084>.
- David C. Flynn and Jim Cannaliato. A new empirical fit to galaxy rotation curves. *Frontiers in Astronomy and Space Sciences*, 12, 2025. doi: 10.3389/fspas.2025.1680387. URL <https://doi.org/10.3389/fspas.2025.1680387>.
- A. E. García Pérez et al. ASPCAP: The APOGEE stellar parameter and chemical abundances pipeline. *AJ*, 151:144, 2016.
- W. E. Harris. A catalog of parameters for globular clusters in the Milky Way. *AJ*, 112:1487, 1996. 2010 revision available at <https://physics.mcmaster.ca/~harris/mwgc.dat>.
- A. Irrgang et al. Milky Way mass models for orbit calculations. *A&A*, 549:A137, 2013.
- I. R. King. The structure of star clusters. III. *AJ*, 71:64, 1966.
- L. Lindegren et al. Gaia Early Data Release 3: The astrometric solution. *A&A*, 649:A2, 2021.
- J. M. D. Kruijssen et al. Kraken reveals itself — the merger history of the Milky Way reconstructed with the E-MOSAICS simulations. *MNRAS*, 498:2472, 2019.
- A. Marín-Franch et al. The ACS survey of Galactic globular clusters. VII. relative ages. *ApJ*, 694:1498, 2009.
- D. E. McLaughlin and R. P. van der Marel. Resolved massive star clusters in the Milky Way and its satellites: Brightness profiles and a catalog of fundamental parameters. *ApJS*, 161:304, 2005. doi: 10.1086/497429.
- R. P. Schiavon et al. The APOGEE value added catalogue of Galactic globular cluster stars. *MNRAS*, 528:1393, 2024. doi: 10.1093/mnras/stad3419.
- A. Sollima, H. Baumgardt, and M. Hilker. The stellar rotation and the kinematic properties of 28 Milky Way globular clusters. *MNRAS*, 485:1460, 2019.

- M. Trenti and R. van der Marel. No energy equipartition in globular clusters. *ApJ*, 775:L2, 2013.
- D. A. Vandenberg et al. The ages of 55 globular clusters as determined using an improved  $\delta v_{\text{TO}}^{\text{HB}}$  method. *ApJ*, 775:134, 2013.
- E. Vasiliev and H. Baumgardt. Gaia EDR3 proper motions of Milky Way globular clusters. *MNRAS*, 505:5978, 2021. doi: 10.1093/mnras/stab1475.